Sample Title: with Forced Linebreak

A. Author,[1, a)] B. Author,[1] and C. Author[2, b)]
[1)] *Authors' institution and/or address*
[2)] *Second institution and/or address*

(*Electronic mail: Second.Author@institution.edu.)

(Dated: 17 March 2024)

An article usually includes an abstract, a concise summary of the work covered at length in the main body of the article. It is used for secondary publications and for information retrieval purposes.

The "lead paragraph" is encapsulated with the LaTeX The lead paragraph will only be found in an article being prepared for the journal *Chaos*.

I. INTRODUCTION

The color of the background represents the order parameter r of the system. The color of the snapshots represents the phase of the oscillators. The color of the arrows represents the direction of the velocity of the oscillators. The size of the arrows represents the speed of the oscillators.

II. MODEL

Oscillators have a spatial position $\mathbf{r}_i = (x_i, y_i)$ and an internal phase θ_i which evoleve according to equations:

$$\dot{x}_i = v\cos\theta_i\,, \tag{1}$$

$$\dot{y}_i = v\sin\theta_i\,, \tag{2}$$

$$\dot{\theta}_i = \omega_i + \lambda\sum_{j=1}^{N} A_{ij}\sin\left(\theta_j - \theta_i\right) \tag{3}$$

for $i = 1, 2, \ldots, N$, where N is the number of oscillators. As per Eq. (1) and (2), each oscillator moves with a constant speed v in the direction of its current phase θ_i. The phase θ_i evolves according to Eq. (3), where ω_i is the natural frequency of the ith oscillator, λ is the coupling strength, and A is the adjacency matrix of the network, with $A_{ij} = 1$ if there is a connection from ith to jth oscillator, and $A_{ij} = 0$ otherwise. We can consider Eq. (1)-(3) as a generalization of the Kuramoto model and the Vicsek model in the sense that it includes both the phase and the spatial position of the oscillators.

Each oscillator i is connected to all the oscillators within a action radius d_0 of its position. The adjacency matrix A is defined as:

$$A_{ij} = \begin{cases} 1, & \left|\mathbf{r}_i - \mathbf{r}_j\right| \le d_0 \\ 0, & \left|\mathbf{r}_i - \mathbf{r}_j\right| > d_0 \end{cases} \tag{4}$$

where $\left|\mathbf{r}_i - \mathbf{r}_j\right|$ is the Euclidean distance between the ith and jth oscillators.

For simplicity, we consider oscillators are initially distributed uniformly in a two-dimensional square with side length L and periodic boundary conditions. Their positions $\mathbf{r}_i\left(t\right) = \left(x_i\left(t\right), y_i\left(t\right)\right)$ at given time t are given by:

$$\begin{aligned} x_i\left(t+\Delta t\right) &= x_i\left(t\right) + v\cos\theta_i\left(t\right)\Delta t \bmod L, \\ x_i\left(t+\Delta t\right) &= x_i\left(t\right) + v\cos\theta_i\left(t\right)\Delta t \bmod L, \end{aligned} \tag{5}$$

where Δt is the discrete time step. When two oscillators are on opposite sides of the square, the absolute value of the difference between one of their coordinates is greater than $L/2$. In this case, we take the minimum distance between them, which is the distance between the two points in the periodic boundary conditions. For a given pair of points $\mathbf{r}_i$ and $\mathbf{r}_j$, the distance between them is $\left|\mathbf{r}_i - \bar{\mathbf{r}}_j\right|$, where $\bar{\mathbf{r}}_j = (\bar{x}_j, \bar{y}_j)$ is the adjusted position of the jth oscillator, given by:

$$\bar{x}_j = \begin{cases} x_j, & \left|x_i - x_j\right| \le L/2 \\ x_j + L, & x_i - x_j > L/2 \\ x_j - L, & x_i - x_j > L/2 \end{cases}, \tag{6}$$

$$\bar{y}_j = \begin{cases} y_j, & \left|y_i - y_j\right| \le L/2 \\ y_j + L, & y_i - y_j > L/2 \\ y_j - L, & y_i - y_j > L/2 \end{cases}. \tag{7}$$

$\left|\mathbf{r}_i - \bar{\mathbf{r}}_j\right|$ can be proved to be the minimum distance between $\mathbf{r}_i$ and $\mathbf{r}_j$ in the periodic boundary conditions (see the proof in Appendix A).

Finally, we consider that the natural frequencies ω_i are distributed in two symmetric uniform distributions. Exactly half of the oscillators have natural frequencies in the range $\left[\omega_{\min}, \omega_{\max}\right]$ $\left(\omega_i \sim U\left(\omega_{\min}, \omega_{\max}\right), i = 1, 2, \ldots, N/2\right)$ and the other half in the range $\left[-\omega_{\max}, -\omega_{\min}\right]$ $\left(\omega_i \sim U\left(-\omega_{\max}, -\omega_{\min}\right), i = N/2+1, N/2+2, \ldots, N\right)$.

III. BEHAVIOR

We performed numerical simulations of the model to probe the behavior of its solutions (see Appendix B for details on the

[a)] Also at Physics Department, XYZ University.
[b)] http://www.Second.institution.edu/~Charlie.Author.

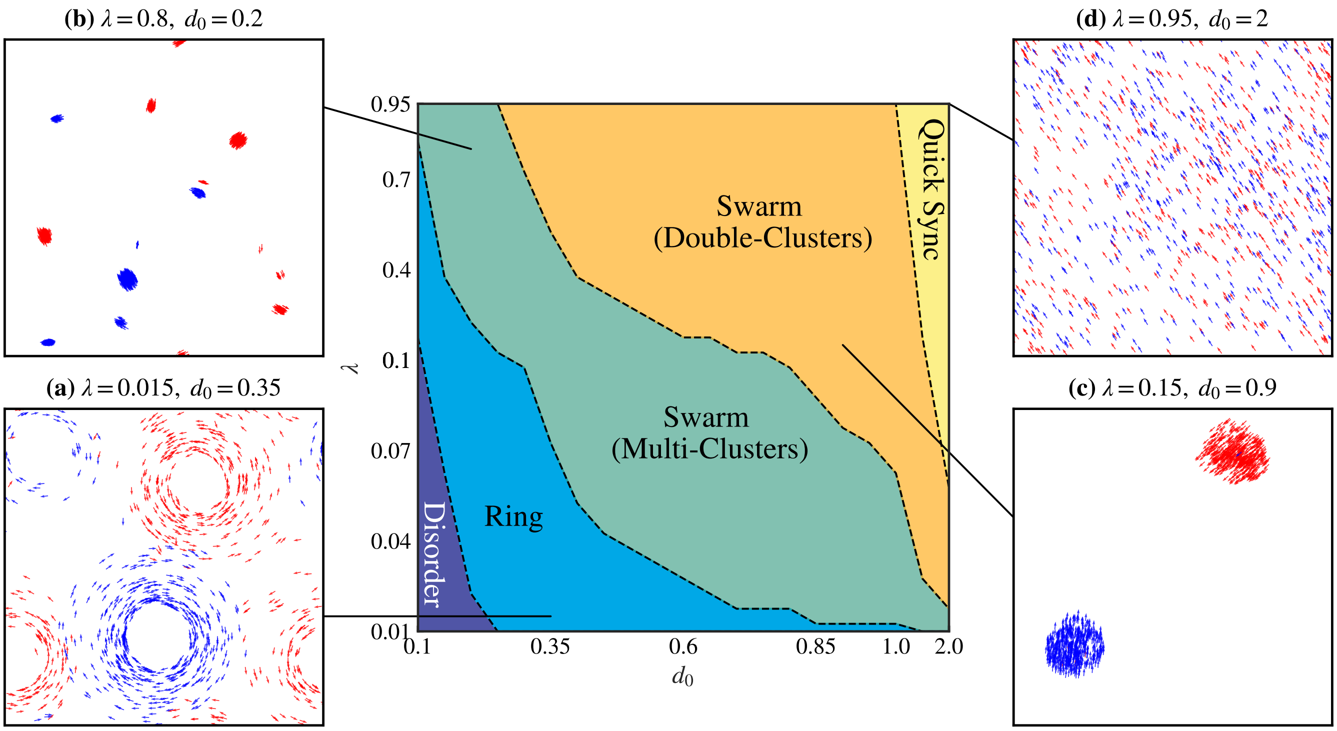

FIG. 1. Phase diagram of model Eq. (1)-(3) in the (λ-d_0) plane. The boundaries between states is analytical approximations given by Section V. For the sake of clarity, the scale of λ and d_0 is non-linear (For λ in $[0.01, 0.1]$ and $[0.1, 1]$, step length is 0.1 and 0.05, respectively. For d_0 in $[0.1, 1]$ and $[1, 2]$, step length is 0.05 and 0.5, respectively). **(a)**, The snapshots of Ring ($\lambda = 0.015,\ d_0 = 0.35$). **(b)**, Swarm (Multi-Clusters) ($\lambda = 0.8,\ d_0 = 0.2$). **(c)**, Swarm (Double-Clusters) ($\lambda = 0.15,\ d_0 = 0.9$). **(d)**, Quick Sync ($\lambda = 0.95,\ d_0 = 2$). Two types of chiral oscillators are represented by red ($\omega_i > 0$) and blue ($\omega_i < 0$) arrows, respectively.

numerical methods). $N = 1000$ oscillators were distributed uniformly in the square of length $L = 10$ and their natural frequencies were distributed in the range $[\omega_{\min}, \omega_{\max}] = [1, 3]$ and $[-\omega_{\max}, -\omega_{\min}] = [-3, -1]$. Two-parameter of coupling strength λ and action radius d_0 are presented in the phase diagram in Fig. 1. We found the system settles into five states: **Disorder**, **Ring**, **Swarm** (which can be further divided into **Multi-Clusters** and **Double-Clusters**), and **Quick Sync**. In Fig. 1 we show the snapshots of the last four states and where these states are located in the phase diagram. We next discuss these five states.

A. Disorder State

Disorder state occurs when both λ and d_0 are small. In this state, the oscillators are not synchronized and move in a way which similar to uncoupled oscillators ($\lambda = 0$), as shown in Fig. 2a. According to Eq. (1)-(3), when $\lambda = 0$, the equations of oscillators' motion can be written as:

$$\begin{aligned} x_i(t) &= x_i(0) + \frac{v}{\omega_i} \sin \omega_i t \ , \\ y_i(t) &= y_i(0) + \frac{v}{\omega_i} \cos \omega_i t \ . \end{aligned} \tag{8}$$

In such a setup, oscillators move in a circular trajectory with a radius v/ω_i and the phase θ_i increases linearly with time, as

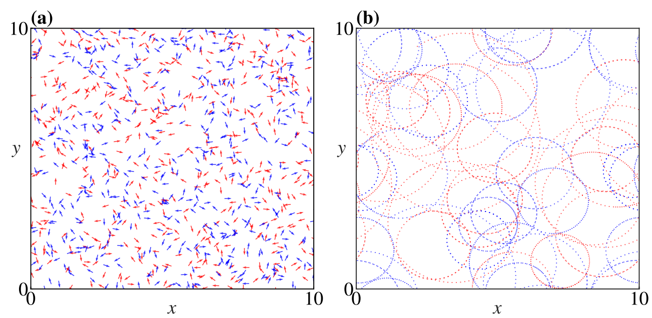

FIG. 2. Key properties of the Disorder state. **(a)**, The snapshot of the Disorder state ($\lambda = 0.01,\ d_0 = 0.1$). **(b)**, The scatter plot of last 100 time steps of 20 positive chirality oscillators and 20 negative chirality oscillators. The plot shows the trajectories are circular.

show in Fig. 2b. To calculate the real-time rotational radius, we first estimate real-time centers $\mathbf{c}(t)$ of the circular trajectory with method in Fig. 3 and then solve the following linear equations:

$$\begin{aligned} \mathbf{c}_i(t_1) \cdot \mathbf{v}_i(t_1) &= \mathbf{x}_i(t_1) \cdot \mathbf{v}_i(t_1) \ , \\ \mathbf{c}_i(t_2) \cdot \mathbf{v}_i(t_2) &= \mathbf{x}_i(t_2) \cdot \mathbf{v}_i(t_2) \ . \end{aligned} \tag{9}$$

The real-time rotational radius is $r_i(t) = |\mathbf{c}_i(t) - \mathbf{r}_i(t)|$. We

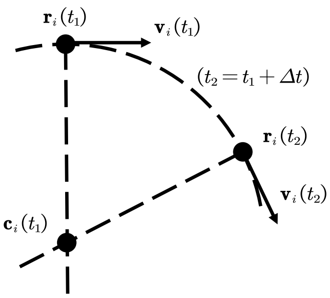

FIG. 3. Estimation for real-time centers. $\mathbf{v}_i(t_1)$ and $\mathbf{r}_i(t_1)$ are the velocity and position of ith oscillator at t_1, respectively. According to Eq. (1)-(3), we can calculate $\mathbf{v}_i(t_2)$ and $\mathbf{r}_i(t_2)$, $(t_2 = t_1 + \Delta t)$. The line $\mathbf{c}_i(t)\mathbf{v}_i(t)$ is perpendicular to $\mathbf{v}_i(t)$. Then we can estimate the real-time center $\mathbf{c}_i(t)$ of the circular trajectory by Eq. (9).

found that the real-time rotational radius is almost constant and close to v/ω_i for each oscillator in the Disorder state, as shown in Fig. 4a.

B. Ring State

The Ring state is characterized by the oscillators forming several rings with thickness, each of which is composed of oscillators with the same chirality, as is show in Fig. 1a. The oscillators in the same ring cluster move in a circular trajectory with a constant rotational radius, as shown in Fig. 4a. There is a long transient time before this state is reached, and in this transient time, the trajectories of oscillators with the same chirality aggregate slowly. Conversely, the trajectories of oscillators with different chirality repel each other, as shown in Fig. 5. For parameter plane in Fig. 1, the number of ring decreases and local swarms appear at high-frequency $(|\omega_i| \to \omega_{\max})$ oscillators with λ and d_0 increasing, as is shown in Fig. 6a.

C. Swarm State

Swarm State is a state where the oscillators align into several clusters, as shown in Fig. 1b and 1c. When λ and d_0 increases, the number of clusters decreases by 2, which is named by as Double-Clusters state, and other states are named by Multi-Clusters state. The clusters are composed of oscillators with the same chirality, and the phase θ_i of the oscillators in the same cluster is synchronized, which means that the oscillators in the cluster move with the same velocity $\mathbf{v}_i = (\cos\theta_s,\, \sin\theta_s)$ and rotational radius $r_i = v/\theta_s$, where θ_s is the oscillators' phase in the cluster. Based on this property, we can calculate θ_s and r_i with Eq. (3):

$$
\begin{aligned}
N_s\omega_s &= \sum_{i=1}^{N_s}\left(\omega_i + \lambda\sum_{j=1}^{N_s} A_{ij}\sin\left(\theta_j - \theta_i\right)\right) \\
\omega_s &= \frac{1}{N_s}\sum_{i=1}^{N_s}\omega_i + \frac{\lambda}{N_s}\sum_{i=1}^{N_s}\sum_{j=1}^{N_s} A_{ij}\sin\left(\theta_j - \theta_i\right) \\
&= \frac{1}{N_s}\sum_{i=1}^{N_s}\omega_i\ ,
\end{aligned}
\tag{10}
$$

where N_s is the number of oscillators in the cluster. As $\omega_i \sim U(\omega_{\min}, \omega_{\max})$ and $\omega_i \sim U(-\omega_{\max}, -\omega_{\min})$ for two types of chirality, we can calculate θ_i, ω_s and r_i with ω_i for Double-Clusters state:

$$
\begin{aligned}
\theta_i = \omega_s &= \begin{cases} \left(\omega_{\max} + \omega_{\min}\right)/2, & i = 1, 2, \ldots, N/2 \\ -\left(\omega_{\max} + \omega_{\min}\right)/2, & i = N/2+1, \cdots, N \end{cases}\ , \\
r_i &= \frac{v}{\omega_s}\ ,
\end{aligned}
\tag{11}
$$

as shown in Fig. 4b. But for Multi-Clusters, due to which oscillators are synchronized within each cluster is not accurately known, we can only calculate the real-time rotational radius of the them. As seen in Fig. 4b, similar to Double-Clusters, some local platforms appear in the real-time rotational radius due to synchronization.

D. Quick Sync State

The Quick Sync state is characterized by the oscillators forming a single cluster, as shown in Fig. 1d. The oscillators in the cluster move with the same velocity and rotational radius, as shown in Fig. 4a. The oscillators in the cluster are synchronized, and the phase θ_i of the oscillators in the cluster is the same, as shown in Fig. **??**.

IV. ORDER PARAMETER

V. ANALYTICAL APPROXIMATIONS

VI. CONCLUSIONS

Appendix A: PROOF OF THE ADJUSTED POSITION

Appendix B: NUMERICAL METHODS

All the simulations of the model Eq. (1)-(3) were run on Python using Euler integration, with a time step $\Delta t = 0.01$, and a total time of $T = 60000$.

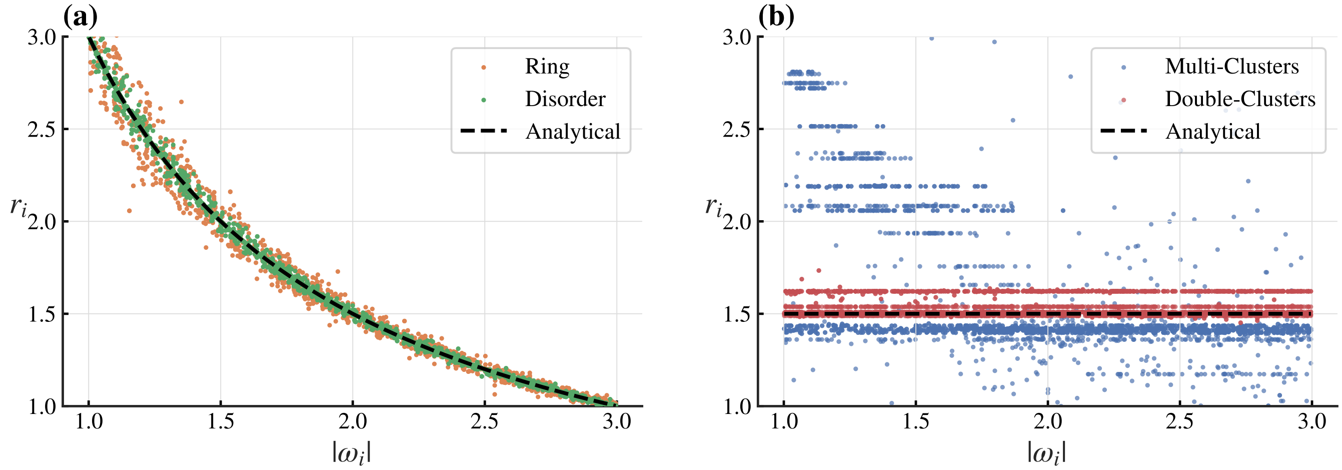

FIG. 4. The real-time and analytical rotational radius. **(a)**, Radius for the Disorder state ($d_0 = 0.1$, $\lambda = 0.01 : 0.06$) and Ring state ($d_0 = 0.1$, $\lambda = 0.06 : 0.1$). The real-time rotational radius is almost constant and close to v/ω_i for each oscillator. **(b)**, Radius for Swarm state (Multi-Clusters, $d_0 = 0.15 : 0.25$, $\lambda = 0.95$) and (Double-Clusters, $d_0 = 2$, $\lambda = 0.02 : 0.05$). Line of Analytical is only for Double-Clusters. All the above simulations are calculated at $t = 60000$.

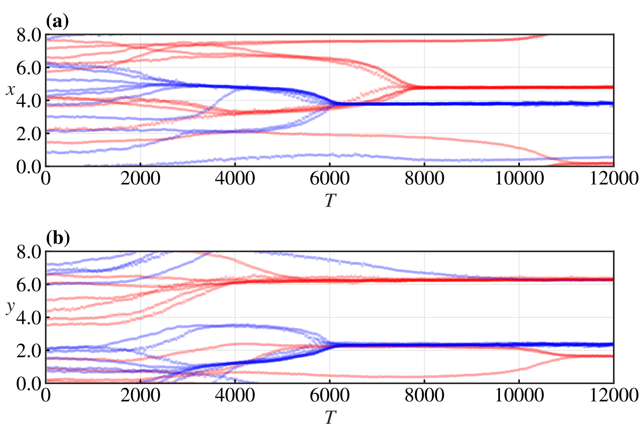

FIG. 5. Scatter plot of the real-time centers position (Ring, $\lambda = 0.02$, $d_0 = 0.4$). **(a)**, horizontal coordinate of centers' positions. **(b)**, vertical coordinate of centers' positions. As time goes on, the centers of oscillators with the same chirality converge.

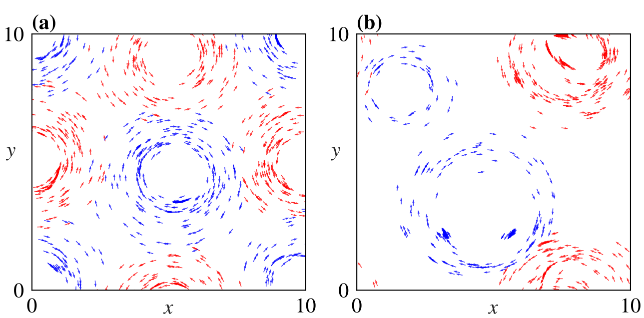

FIG. 6. Scatter plot of the real-time centers position (Ring, $\lambda = 0.02$, $d_0 = 0.4$). **(a)**, horizontal coordinate of centers' positions. **(b)**, vertical coordinate of centers' positions. As time goes on, the centers of oscillators with the same chirality converge.